Article type : Research Article

A Cyanine Photooxidation/β-Elimination Sequence Enables Near-Infrared Uncaging of Aryl Amine Payloads

Tsuyoshi Yamamoto,[1a] Donald R. Caldwell,[1] Albert Gandioso,[1,2] Martin J. Schnermann[1**]

[1]Chemical Biology Laboratory, Center for Cancer Research, National Cancer Institute Frederick, MD 21702 (USA)

[2] Seccio de Química Orgànica ,Departament de Química Inorganica i Organica ,Universitat de Barcelona, Martí i Franques 1-11, E-08028 Barcelona, Spain

[a] Current address: Graduate School of Biomedical Sciences, Nagasaki University Nagasaki, 852-8521 (JAPAN)

*Corresponding author e-mail: martin.schnermann@nih.gov

ABSTRACT

Uncaging strategies that use near-infrared (NIR) wavelengths can enable the highly targeted delivery of biomolecules in complex settings. Many methods, including an approach we developed using cyanine photooxidation, are limited to phenol-containing payloads. Given the critical role of amines in diverse biological processes, we sought to use cyanine photooxidation to initiate the release of aryl amines. Heptamethine cyanines substituted with an aryl amine at the C4' position undergo only inefficient release, likely due electronic factors. We then pursued the hypothesis that the carbonyl products derived from cyanine photooxidation could undergo efficient β-elimination. After examining both symmetrical and unsymmetrical scaffolds, we identify a merocyanine substituted with indolenine and coumarin heterocycles that undergoes efficient photooxidation and aniline uncaging. In total, these studies provide a new scheme – cyanine photooxidation followed by β-elimination – through which to design photocages with efficient uncaging properties.

INTRODUCTION

The photocaged/uncaged paradigm is a useful manifold to modulate biological function with high spatial and temporal control (1, 2). To transition these experiments into increasingly complex physiological environments, photocages activated with single photon flux of far-red and near-infrared wavelengths would be highly enabling. Recent efforts have identified some of the first useful small molecule-based methods in this range. Given the modest photonic energies of these wavelengths, it is not surprising that these approaches employ a range of chemical mechanisms for bond cleavage (3). These include the direct cleavage of certain chromophore-payload bonds, the cleavage of carbon-metal bonds, the use of photoinduced electron transfer (PET)-mediated processes, and the local

generation of singlet oxygen ($^1O_2$) (4-12)(13). Despite progress, significant reaction discovery efforts are needed to uncover methods characterized by broad payload flexibility, activation with wavelengths over 700 nm, and rapid release.

Our group has sought to use cyanine photooxidation as a triggering event to initiate uncaging (14-16). Molecules of the general type shown in Figure 1A undergo $^1O_2$-mediated oxidative cleavage between the C2/C1' and C2'/C3' positions and then a hydrolysis/cyclization cascade to liberate phenol payloads (17). The key element of this approach is the altered hydrolytic stability of the C4'-N bond following oxidative cleavage. We have applied this approach to create NIR-activated antibody-drug conjugates that release potent anti-tumor agents with *in vivo* activity (18, 19). Given the critical role that nucleic acids and other amine-containing molecules play in biological processes (20, 21), NIR uncaging strategies that release amine payloads have broad potential impact.

Here we detail efforts to apply cyanine photooxidation as an initiating event for amine uncaging. We find that the direct attachment of aniline payloads to the C4' position of the heptamethine cyanine leads to only inefficient release under physiological conditions (Figure 1B). We then considered whether the oxidative formation of carbonyl products could be harnessed to initiate a β-elimination event. We prepared derivatives, including a symmetrical heptamethine cyanine and unsymmetrical merocyanines, with suitably positioned carbamate functional groups. Through this approach, we identify a merocyanine that is highly water soluble and undergoes efficient photooxidiation with useful uncaging yields.

<figure 1>

MATERIALS AND METHODS

Reagents. Unless stated otherwise, reactions were conducted in oven-dried glassware under an atmosphere of argon using anhydrous solvents (passed through activated alumina columns). All commercially obtained reagents were used as received. Flash column chromatography was performed using reversed phase (100 Å, 20-40 micron particle size, RediSep® Rf Gold® Reversed-phase C18 or C18Aq) on a CombiFlash® Rf 200i (Teledyne Isco, Inc., Lincoln, NE).

Apparatus. High-resolution LC/MS analyses were conducted on a Thermo-Fisher LTQ-Orbitrap-XL hybrid mass spectrometer system with an Ion MAX API electrospray ion source in negative ion mode. Analytical LC/MS was performed using a Shimadzu LCMS-2020 Single Quadrupole utilizing a Kinetex 2.6 μm C18 100 Å (2.1 x 50 mm) column obtained from Phenomenex, Inc (Torrance, CA). Runs employed a gradient of 0-90% MeCN/0.1% aqueous formic acid over 4.5 min at a flow rate of 0.2 mL/min. ^{1}H-NMR and ^{13}C-NMR spectra were recorded on Bruker spectrometers (at 400 or 500 MHz or at 100 or 125 MHz) and are reported relative to deuterated solvent signals. Data for ^{1}H-NMR spectra are reported as follows: chemical shift (δ ppm), multiplicity, coupling constant (Hz), and integration. Data for ^{13}C-NMR spectra are reported in terms of chemical shift. Absorbance curves were obtained on a Shimadzu UV-2550 spectrophotometer operated by UVProbe 2.32 software. Samples in 96-well plates (Corning black plate, clear bottom, polystyrene, #3603) were irradiated using a 690 ± 20 nm LED (L690-66-60, Marubeni America Co.) at a light intensity of 20 mW/cm2 as measured using a power meter. Fluorescence traces were recorded on a PTI QuantaMaster steady-state spectrofluorimeter operated by FelixGX 4.2.2 software, with 5 nm excitation and emission slit widths, and a 0.1 s integration rate. Data analysis and curve fitting were performed using MS Excel 2011 and GraphPad Prism 7.

Synthesis of Cy7-C4-Cou. In a glove-box, IR-783 (100 mg, 0.13 mmol), 7-amino-4-(trifluoromethyl)chromen-2-one, Coumarin 151 (42.8 mg, 0.19 mmol), $Pd_2(dba)_3$•$CHCl_3$ (12 mg, 0.013 mmol), BrettPhos (14.5 mg, 0.026 mmol), Cs_2CO_3 (87 mg, 0.26 mmol) and *N,N*-dimethylformamide (2 mL) were added to an oven dried microwave and the vial was sealed. The resulting heterogenous mixture was heated to 80 ºC and vigorously stirred for 1 h under inert atmosphere, after which time LC/MS analysis of the reaction showed completed consumption of IR-783. The reaction was cooled to room temperature and filtered through celite. The flow-through was diluted with water (3 mL) subjected to reverse-phase column chromatography (C_{18}, 20–60% MeCN/H_2O). The solvent was removed *in vacuo* to afford Cy7-C4-Cou (71 mg, 57% yield) as a green solid. ^{1}H NMR (DMSO-d_6, 500 MHz) δ 9.26 (s, 1H), 7.90 (d, *J* = 14.1 Hz, 2H), 7.57 (d, *J* = 8.1 Hz, 1H), 7.48 (d, *J* = 7.3 Hz, 2H), 7.39–7.33 (m, 4H), 7.17 (t, *J* = 7.7 Hz, 2H), 6.94 (br, 1H), 6.77 (br, 1H), 6.60 (s, 1H), 6.25 (d, *J* = 14.1 Hz, 2H), 4.13 (br, 4H), 2.71 (br, 4H),1.93 (br, 4H), 1.80–1.67 (m, 8H), 1.32 (s, 12H); ^{13}C NMR (DMSO-d_6, 125 MHz) δ 171.63, 159.40, 156.82, 153.04, 152.97, 142.63, 142.35, 141.33, 140.20 (q, *J* = 30.9 Hz), 128.90, 127.05, 126.67, 124.95, 123.35, 122.77, 121.16, 112.57, 111.62, 110.47, 104.14, 100.82, 100.39, 72.96, 63.54, 51.23, 48.93, 43.97, 27.74, 26.48, 24.51, 23.00, 21.38; HRMS (ESI) calculated for $C_{48}H_{53}F_3N_3O_8S_2$ (M^+) 920.3221, observed 920.3200.

*Synthesis of **4***. At 0 ºC, phosphorous oxychloride (1.12 g, 7.32 mmol) was added dropwise to anhydrous DMF (1.37 mL, 17.7 mmol). After stirring for 30 min, 4-hydroxy-cyclohexanone, **1**, (186 mg, 1.62 mmol) in anhydrous DMF (1 mL, 14.5 mmol) was added dropwise to the reaction at 0 ºC and the mixture was heated at 50 ºC for 1 h in an oil bath. A mixture of aniline/ethanol (50% v/v, 4 mL) was then added dropwise to the mixture at room temperature. The resulting mixture was poured into ice-cold conc. HCl (10:1 v/v, 22 mL). The mixture was allowed to stand for 5 h at –4 ºC and then the formed solid was filtrated off, washed with cold water, ethanol and diethyl ether, and then dried *in vacuo* to afford chloride **2** as a purple solid (332 mg). The solid was used without further purification. To a 20-mL vial was added indoleine **3** (500 mg, 1.69 mmol),(22) chloride **2** (192

mg, 0.57 mmol), sodium acetate (232 mg, 2.80 mmol), ethanol (2 mL) in succession. Acetic anhydride (286 mg, 2.80 mmol) was added and the reaction was stirred at room temperature for 2 h. The reaction was precipitated into ether (50 mL), the slurry was centrifuged at 3,500 rpm for 5 min and the supernatant was discarded. This procedure was repeated twice. The crude solid was placed under vacuum for 1 h, and the solid was dissolved in H_2O (3 mL). The mixture was subjected to reverse-phase chromatography (C_{18} column, 0 to 100% MeCN/H_2O). The solvent was removed *in vacuo* to afford **4** (110 mg, 25% yield) as a green solid. ^{1}H NMR (Methanol-d_4, 500 MHz) δ8.51 (d, *J* = 14.3 Hz, 2H), 7.54 (d, *J* = 7.4 Hz, 2H), 7.47–7.40 (m, 4H), 7.30 (t, *J* = 7.43 Hz, 2H), 4.30 (m, 1H), 4.25 (t, *J* = 7.51 Hz, 4H), 2.98 (dd, *J* = 15.7, 4.0 Hz, 2H), 2.92 (t, *J* = 6.9 Hz, 4H), 2.78 (dd, *J* = 15.7, 6.9 Hz, 2H), 2.0 (m, 8H), 1.76 (s, 12H); ^{13}C NMR (Methanol-d_4, 125 MHz) δ173.00, 148.92, 145.05, 142.21, 141.24, 128.53, 125.13, 123.75, 122.04, 111.06, 101.08, 63.53, 50.33, 49.29, 48.10, 43.66, 33.66, 26.91, 25.89, 22.22. HRMS (ESI) calculated for $C_{38}H_{48}ClN_2O_7S_2$ (M^+) 743.2586, observed 743.2570.

Synthesis of Cy7-β-Cou. To a 25-mL pear-shaped flask was added 7-amino-4-(trifluoromethyl)chromen-2-one (100 mg, 0.44 mmol) and phosgene solution (3 mL, 4.9 mmol; 15%wt in toluene) at room temperature. The mixture was stirred for 20 min at room temperature and then heated to 80 ºC for 13 h. The reaction was cooled and the solvent and excess phosgene was removed *in vacuo* to afford **6**, which was used without further purification. To the resulting solid was added a mixture of **4** (20 mg, 26 µmol), dichloromethane/*N*-methyl-2-pyrrolidone (50%v/v) and *N,N*-diisopropylethylamine (45 µL, 0.26 mmol) at 0 ºC. The reaction was stirred for 1 h in an ice bath and then precipitated in ether (50 mL). The slurry was centrifuged at 3,500 rpm for 5 min and the supernatant was discarded. This procedure was repeated twice. The crude solid was placed under vacuum for 1 h, and the solid was dissolved in H_2O/MeCN (3 mL, 50% v/v). The mixture was subjected to reverse-phase chromatography (C_{18} column, 0 to 100% MeCN/H_2O). The solvent was removed in vacuo to afford Cy7-β-Cou (20 mg, 76% yield) as a green solid. ^{1}H NMR (Methanol-d_4, 500 MHz) δ8.53 (d, *J* = 14.2 Hz, 2H), 7.74 (s, 1H), 7.62 (d, *J* = 8.6 Hz, 1H), 7.54 (d, *J* = 7.6 Hz, 2H),

7.46–7.39 (m, 5H), 7.31 (t, *J* = 7.1 Hz, 2H), 6.72 (s, 1H), 6.38 (d, *J* = 14.3, 2H), 5.49 (br, 1H), 4.26 (t, *J* = 7.3 Hz, 4H), 3.24–3.02 (m, 4H), 2.89 (t, *J* = 7.3 Hz, 4H), 2.08–1.90 (m, 8H), 1.76 (d, *J* = 7.19 Hz, 12H); ^{13}C NMR (Methanol-d_4, 125 MHz) δ 173.34, 159.41, 155.42, 153.27, 148.39, 144.97, 144.06, 142.17, 141.29, 140.76 (q, *J* = 32.6 Hz), 128.56, 125.33, 125.26, 122.23, 122.05, 115.01, 113.01, 112.96, 111.22, 107.92, 105.36, 101.10, 67.94, 50.37, 49.39, 43.75, 30.78, 26.93, 26.90, 25.96, 22.18. HRMS (ESI) calculated for $C_{49}H_{52}ClF_3N_3O_{10}S_2$ (M^+) 998.2729, observed 998.2711.

Synthesis of ***9***. To a round-bottom flask was added dichloromethane (30 mL) and pyridine (218 µL, 2.7 mmol). After the mixture was cooled to –78 ºC, glycidol (140 µL, 2.7 mmol) and trifluoromethanesulfonic anhydride (454 µL, 2.7 mmol) were added dropwise in succession to the mixture. The reaction was stirred at –78 ºC for 40 min and was warmed to room temperature. To the mixture was added hexane (30 mL) and the resulting suspension was subjected to short silica gel column chromatography (10 g of silica gel with 30 mL of dichloromethane). The solvent was removed *in vacuo* and the resulting clear oil was used without further purification. To this oil was added dichloromethane (10 mL) under inert atmosphere. After the mixture was then cooled to –78 ºC, 2,3,3-trimethylindolenine, **7**, (216 µL, 1.35 mmol) and *N*,*N*-diisopropylethylamine (235 µL, 1.35 mmol) were added to the solution in succession. The reaction was stirred at –78 ºC for 20 min and then warmed up to room temperature over 1 h. The reaction was directly subjected to silica gel column chromatography (0–30% MeOH/DCM). The solvent was removed to afford **9** as a clear oil (215 mg, 75% yield). ^{1}H NMR (Chloroform-*d*, 400 MHz) δ 7.82–7.77 (m, 1H), 7.56–7.48 (m, 3H), 5.06 (d, *J* = 15.1 Hz, 1H) 4.42 (dd, *J* =15.1, 6.6 Hz, 1H), 3.49 (m, 1H), 2.87 (t, *J* = 4.3 Hz, 1H), 2.63 (dd, *J* = 4.4, 2.5 Hz, 1H), 1.53 (d, *J* = 3.6 Hz, 6H); ^{13}C NMR (Chloroform-*d*, 100 MHz) δ 198.89, 141.26, 141.16, 130.14, 129.55, 123.15, 115.59, 54.88, 49.91, 48.72, 45.72, 22.79, 22.68, 14.65; HRMS (ESI) calculated for $C_{14}H_{18}NO^+$ (M^+) 216.1383, observed 216.1378.

*Synthesis of **10**.* To a round-bottom flask was added **9** (670 mg, 3.1 mmol) and dichloromethane (30 mL). To the mixture was added trifluoromethanesulfonic acid (603 µL, 6.8 mmol). The reaction was stirred for 20 h at room temperature. The resulting solution was washed with saturated sodium bicarbonate aqueous solution (40 mL) and brine (40 mL). The organic layer was dried over Na_2SO_4, added formic acid (500 µL) and the solvent was removed *in vacuo*. The resulting oil was subjected to reverse-phase column chromatography (C_{18}, 0–100% MeCN/H_2O). The solvent was removed *in vacuo* to afford **10** as a clear oil (476 mg, 71% yield). ^{1}H NMR (Methanol-d_4, 500 MHz) δ 7.80–7.76 (m, 2H), 7.67–7.63 (m, 2H), 4.59 (m, 1H), 4.43–4.34 (m, 2H), 2.23–2.12 (m, 2H), 1.63 (d, J = 21.8 Hz, 6H); ^{13}C NMR (Methanol-d_4, 126 MHz) δ 195.51, 141.93, 141.79, 129.86, 128.96, 122.96, 114.14, 60.44, 53.67, 51.78, 23.26, 21.86, 21.41, 19.38; HRMS (ESI) calculated for $C_{14}H_{18}NO^+$ (M^+) 216.1383, observed 216.1380.

*Synthesis of **13**.* In a round-bottom flask was added *N*-[5-(phenylamino)-2,4-pentadienylidene]aniline monohydrochloride, **11**, (0.50 g, 1.75 mmol), 1,3-dimethyl barbituric acid, **12**, (0.27 g, 1.75 mmol), sodium acetate (0.14 g, 1.75 mmol) and acetic anhydride (2.5 mL). The flask was evacuated and flushed with argon. The reaction was stirred at 160 °C for 5 min as the solution color transitioned from dark red to dark brown. The reaction mixture was cooled and concentrated with 2 g of SiO_2 and then purified by normal phase chromatography (80 g silica column, 0-80% EtOAc/Hexane) to afford **13** (0.23 g, 37% yield) as a dark brown solid. ^{1}H NMR (Chloroform-d_1, 500 MHz) δ 8.16 (d, J = 13.9 Hz, 1H), 8.04 (d, J = 12.5 Hz, 1H), 7.70 (dd, J = 14.4, 12.4 Hz, 1H), 7.59 – 7.52 (m, 3H), 7.23 – 7.18 (m, 3H), 5.40 (dd, J = 13.7, 11.4 Hz, 1H), 3.35 (s, 3H), 3.30 (s, 3H), 1.97 (s, 3H); ^{13}C NMR (Chloroform-*d*, 125 MHz) δ 169.24, 162.60, 161.95, 157.18, 154.95, 151.59, 140.76, 138.23, 130.59, 129.75, 128.29, 126.76, 113.75, 111.60, 28.57, 27.87, 23.37; HRMS (ESI) calculated for $C_{19}H_{20}N_3O_4$ (MH^+) 354.1448, observed 354.1444.

Synthesis of BI-β-Cou. To a microwave vial was added **10** (60 mg, 0.27 mmol), **13** (75.7 mg, 0.21 mmol), sodium acetate (46 mg, 0.56 mmol) and MeOH/DCM (2 mL, 50% v/v) in succession. The vial was sealed and heated with a microwave reactor to 75 °C for 1 h as the solution color transitioned from dark red to blue. The reaction mixture was cooled and concentrated with 0.5 g of silica gel and then purified by normal phase chromatography (12 g silica column, 0–100% ethyl acetate/hexane) to afford the intermediate merocyanine as a dark blue solid, which was immediately used for the next. The intermediate merocyanine in dichloromethane (3 mL) was added to **6** (0.22 mmol, generated as above) at 0 °C. After addition of *N*,*N*-diisopropylethyamine (38 µL, 0.22 mmol) at 0 ºC, the reaction was stirred for 30 min in an ice bath. Then the reaction was warmed to room temperature and stirred for 3 h. The reaction mixture was concentrated and purified by normal–phase chromatography (12 g of silica gel, 0–100% EtOAc/hexane) to afford *BI-β-Cou* (28 mg, 19% yield) as a dark blue solid. ^{1}H NMR (Chloroform-*d*, 500 MHz,) δ 8.05 (d, *J* = 12.7 Hz, 1H), 7.85 (t, *J* = 13.7 Hz, 1H), 7.67 (s, 1H), 7.62 (d, *J* = 8.7 Hz, 1H), 7.49–7.45 (m, 2H), 7.32–7.25 (m, 4H), 7.06 (t, *J* = 7.2 Hz, 1H), 6.80 (d, *J* = 8.7 Hz, 1H), 6.66 (s, 1H), 6.29 (t, *J* = 13.0 Hz, 1H), 5.53 (br, 1H), 3.99 (d, *J* = 13.4 Hz, 1H), 3.88 (d, *J* = 13.0 Hz, 1H), 3.33 (d, *J* = 17.4 Hz, 6H), 2.78 (s, 2H), 1.66 (s, 6H); ^{13}C NMR (Chloroform-*d*, 125 MHz) δ 163.27, 162.44, 160.36, 159.15, 156.81, 155.42, 151.99, 151.94, 144.53, 142.68, 142.20, 141.28 (q, *J* = 33.1 Hz, CF_3), 139.52, 128.25, 126.12, 124.38, 122.68, 122.56, 122.00, 120.37, 120.08, 115.21, 113.66, 109.04, 107.49, 107.36, 106.31, 102.31, 65.96, 47.30, 44.90, 28.75, 28.58, 28.42, 27.74; HRMS (ESI) calculated for $C_{36}H_{32}F_3N_4O_7$ (MH^+) 689.2218, observed 689.2216.

*Synthesis of **15***. To a round-bottom flask was added *N*,*N*-dimethylformamide (2 mL, 25.8 mmol). After cooled to 0 ºC, phosphoryl chloride (298 µL, 3.20 mmol) was added dropwise over 5 min. The reaction was then warmed to room temperature and stirred for 30 min. The reaction was cooled to 0 ºC again and added 2-[6-(diethylamino)-2,3-dihydro-1H-xanthen-9-yl]-benzoic acid **14** (400 mg, 1.07 mmol)(23) in *N*,*N*-dimethylformamide (2 mL) dropwise under 0 ºC. The reaction was stirred for 10 min at 0 ºC and for 1 h at room temperature. The reaction was cooled to 0 ºC and quenched with H_2O (2 mL) and stirred at room temperature for 3 d. The resulting solution was subjected to reverse-phase

chromatography (C_{18}, 5–100% MeCN/H_2O). The solvent was removed *in vacuo* to afford aldehyde **15** (356 mg, 82% yield). ^{1}H NMR (DMSO-d_6, 400 MHz) δ 10.29 (s, 1H), 8.05 (dd, *J* = 1.3, 7.9 Hz, 1H), 7.70 (dt, *J* = 1.4, 7.5 Hz, 1H), 7.58 (dt, *J* = 1.4 and 7.6 Hz, 1H) , 7.24 (dd, *J* = 7.6, 1.1 Hz, 1H), 6.57 (d, *J* = 2.4 Hz, 1H), 6.39 (dd, *J* =9.0, 2.4 Hz, 1H), 6.32 (d, *J* = 9.0 Hz, 1H), 3.36 (q, *J* = 7.0 Hz, 4H), 2.27 (t, *J* = 6.0 Hz, 2H), 2.17–2.02 (m, 2H), 1.58–1.44 (m, 2H), 1.09 (t, *J* = 7.1 Hz, 6H);^{13}C NMR (DMSO-d_6, 100 MHz) *δ* 186.07, 167.65, 161.66, 153.46, 149.59, 140.87, 136.37, 132.81, 131.70, 130.81, 130.40, 128.95, 126.79, 118.61, 111.21, 110.93, 108.25, 97.11, 44.31, 27.39, 21.65, 20.50, 12.92, 12.73. HRMS (ESI) calculated for $C_{25}H_{26}NO_4$ (MH^+) 404.1856, observed 404.1850.

Synthesis of Cl-β-Cou. To a 20-mL vial was added **15** (292 mg, 0.68 mmol), **10** (220 mg, 1.02 mmol), sodium acetate (342 mg, 4.07 mmol), ethanol (5 mL) and acetic anhydride (451 µL, 4.07 mmol) in succession. The reaction was heated at 100 ºC for 2 h. After cooled to room temperature, ethyl acetate (50 mL) was added to the reaction and the organic layer was washed with saturated sodium bicarbonate solution (30 mL × 2) and brine (30 mL × 2). The organic layer was dried over Na_2SO_4 and concentrated *in vacuo*. To the resulting solid was added sodium iodide (4g) in H_2O/MeOH/DCM (4 mL/1 mL/3 mL) and the solution was stirred for 8 h. To the mixture was added dichloromethane (30 mL) and the solution was washed with H_2O (30 mL). The resulting organic layer was dried over Na_2SO_4 and concentrated in vacuo. The crude mixture was purified by silica gel chromatography (40 g of silica gel, 0–100% MeOH/dichloromethane) to afford the intermediate secondary alcohol as a green solid (170 mg, 34% yield). ^{1}H NMR (Methanol-d_4, 400 MHz) δ 8.63 (s, 1H), 8.01–7.97 (m, 1H), 7.57–7.51 (m, 3H), 7.43 (t, *J* = 7.7 Hz, 1H), 7.29 (t, *J* = 7.3 Hz, 1H), 7.24 (d, *J* = 7.9 Hz, 1H), 7.15–7.11 (m, 1H), 6.94 (dd, *J* = 9.1, 3.7 Hz, 1H), 6.80–6.76 (m, 1H), 6.63 (br, 1H), 4.49–4.42 (m, 1H), 4.04–3.93 (m, 2H), 3.57 (q, *J* = 7.1 Hz, 4H), 3.12 (d, *J* = 3.3 Hz, 2H), 2.99–2.89 (m, 2H), 2.55–2.32 (m, 2H), 1.88 (dd, *J* = 14.8, 2.4 Hz, 6H), 1.83 (br, 2H), 1.28 (t, *J* = 7.3 Hz, 6H); ^{13}C NMR (Methanol-d_4, 100 MHz) δ 173.07, 170.63, 164.09, 155.89, 154.29, 151.67, 142.54, 142.44, 140.94, 139.72, 133.74, 129.26, 129.02, 128.85, 128.32, 128.16, 124.64, 121.96, 120.93, 114.39, 113.66, 111.69, 109.54, 108.86,

94.89, 61.13, 49.09, 44.68, 32.53, 27.90, 27.38, 26.93, 26.36, 21.30, 11.27; HRMS (ESI) calculated for $C_{39}H_{41}N_2O_4^+$ (M^+) 601.3061, observed 601.3034. To **6** (0.17 mmol, generated as above) was added the intermediate above (20 mg, 0.033 mmol), dichloromethane and *N,N*-diisopropylethylamine (45 µL, 0.26 mmol) in succession at 0 ºC. After the reaction was stirred for 1 h in an ice bath, the bath was removed and for 12 h. To the reaction was added dichloromethane (50 mL) and washed with saturated aqueous $NaHCO_3$ solution (50 mL × 2) and brine (50 mL × 2). The organic layer was dried over Na_2SO_4 and the solvent was removed *in vacuo*. The mixture was subjected to quick silica gel chromatography (24 g of silica gel, 30–100% hexane/ethyl acetate, and then 0–100% MeOH/DCM). The solvent was removed *in vacuo* to afford a green solid. The solid was dissolved in H_2O/MeOH (50% v/v, 8 mL) and then sodium iodide (3 g) was added. The colored mixture was stirred for 16 h under a light–shielded condition. To the solution was added dichloromethane (50 mL) and washed with H_2O (50 mL). The organic layer was dried over Na_2SO_4 and the solvent was removed *in vacuo*. Purification by silica gel chromatography was performed (24 g of silica gel, 30–100% hexane/ethyl acetate, and then 0–100% MeOH/DCM). The solvent was removed *in vacuo* to obtain Cl-β-Cou (20 mg, 62% yield) as a green solid. ^{1}H NMR (Methanol-d_4, 500 MHz) δ 8.62 (s, 1H), 8.05 (d, *J* = 7.8 Hz, 1H), 7.71 (br, 1H), 7.62–7.54 (m, 4H), 7.42 (t, *J* = 7.6 Hz, 1H), 7.38–7.23 (m, 3H), 7.15 (d, *J* = 7.1 Hz, 1H), 6.91 (d, *J* = 9.1 Hz, 1H), 6.81 (d, *J* = 8.8 Hz, 1H), 6.70 (s, 1H), 6.63 (s, 1H), 5.58 (br, 1H), 4.26 (dd, *J* = 14.7 and 70.4 Hz, 2H), 3.58 (q, *J* = 7.0 Hz, 4H), 3.45 (d, *J* = 16.0 Hz, 1H), 3.32 (quint, *J* = 1.7 Hz, 4H), 3.24 (d, J = 16.0 Hz, 1H), 3.30–2.84 (m, 2H), 2.46–2.33 (m, 2H), 1.91 (d, *J* = 14.8 Hz, 6H), 1.77–1.65 (br, 2H), 1.28 (t, *J* = 7.1 Hz, 6H); ^{13}C NMR (Methanol-d_4, 125 MHz) δ 169.72, 164.24, 159.28, 156.07, 155.36, 155.04, 152.77, 152.01, 143.72, 142.25, 141.88, 140.83, 140.62, 140.51, 134.28, 129.99, 129.84, 128.80, 128.60, 128.38, 128.33, 125.33, 124.59, 123.12, 122.04, 121.01, 120.39, 114.97, 114.81, 113.76, 113.21, 113.15, 112.17, 109.35, 108.09, 107.25, 105.49, 94.85, 65.34, 49.10, 45.85, 44.76, 29.54, 28.06, 27.38, 26.93, 26.04, 21.20, 11.27. HRMS (ESI) calculated for $C_{50}H_{45}F_3N_3O_7^+$ (M^+) 856.3204, observed 856.3160.

Procedure for Determining Photooxidation Efficiency and Uncaging Kinetics. Stock solutions of the coumarin 151 conjugates Cy7-C4-Cou, Cy7-β-Cou, BI-β-Cou, and CI-β-Cou were diluted into 5% DMSO/pH 7.4 PBS (50 mM) to afford 2 μM solutions. Samples were dispensed into 96-well plates (Corning black plate, clear bottom, polystyrene, #3603) and sealed with ThermalSeal RT film (Sigma, Z707465). Samples in the 96-well plate were irradiated using a 780 LED ± 20 nm (L780-66-60, Marubeni America Co.) for Cy7-C4-Cou and Cy7-β-Cou, 690 nm LED (L690-66-60, Marubeni America Co.) for BI-β-Cou and 740 nm LED (L740-66-60, Marubeni America Co.) for CI-β-Cou at a light intensity of 20 mW/cm^2 as measured using a power meter. Single point absorption measurements at the λ_{max} and Coumarin 151 fluorescence (ex 372 nm, em 490 nm) were recorded at regular intervals (1-30 minutes for 12-150 minutes depending on photobleaching rate) until ablation of the absorbance signal. Experiments were run in quadruplicate and plotted with error bars derived from the standard deviation (<5% in all cases). Half-lives were obtained by fitting the curves with one phase decay parameters in all cases except for CI-β-Cou, for which two phase decay parameters were used. Percent yield of Coumarin 151 release was obtained from the input of the experimental fluorescence values into the equation derived from the standard calibration curve, with 2 μM defined as 100% yield (Figure S1).

Procedure for LC/MS Relative Ion Analysis of Cy7-β-Cou Photolysis. A 10 mM stock of Cy7-β-Cou in DMSO was diluted into water to yield a 10 uM solution. Phenylalanine (40 uM) was used as an internal standard. The photolysis was run for 1 h at 23 ºC with 20 mW/cm^2 780 ± 20 nm light in a 2 mL vial without a cap. After 1 h, the reaction was capped and keep in the dark. Aliquots were taken at 0 (prior to irradiation), 1 h, 2 h, 6 h, and 14 h and immediately analyzed by a direct loop injection method with a Shimadzu LCMS-2020 Single Quadrupole instrument (normal resolution) The relative ion counts in Figure 3C were calculated by integrating the extracted ion chromatogram (EIC) of the m/z of Cy7-β-Cou, Int-1 + Int-1-H_2O, Int-2, and C151 and dividing by the ion count of phenylalanine internal standard.

RESULTS

Based on our prior studies (Figure 1A), a straightforward approach to this problem entails the direct attachment of the aniline-containing substrate onto the C4' position of the heptamethine scaffold. The preparation of the corresponding aniline-modified cyanines proceeds readily through a Pd(0)-mediated arylation reaction to provide Cy7-C4-Cou directly from the corresponding C4'-chloro IR-783 (Figure 2A). The optical properties of Cy7-C4-Cou are consistent with previously prepared C4' *N*-arylated cyanines (Table 1) (24).

<figure 2>

<figure 3>

Photooxidation of Cy7-C4-Cou using a 780 nm LED (20 mW/cm^2) in pH 7.4 PBS w/5% DMSO proceeds efficiently, with similar kinetics to our prior efforts ($t_{1/2}$ = 5.7 min, Figure 3B). However, irradiation leads to only barely detectable release of the fluorescent coumarin 151 at rt over 1 h (<1 %, Figure S2). When Cy7-C4-Cou is subjected to complete photooxidation at rt and then incubated at 37 °C, modest release occurs over a 24 h time frame (8% vs <1% without irradiation, Figure 3B, see Figure S3 for background release curves). These results suggest that C4' aniline-substituted cyanines will only be useful for uncaging applications requiring slow release of the payload.

We then set out to identify an approach characterized by rapid kinetics. Our prior efforts were based on the premise that cyanine photooxidation alters the electronic structure of the cyanine scaffold, thereby enhancing the rate of C4'-N hydrolysis. Another feature of photooxidation is the formation of a carbonyl product. Release strategies using a carbonyl formation/β-elimination manifold have been reported in several contexts, leading us to consider if similar logic could be

applied here. (25-28) As an initial entry, we generated Cy7-β-Cou through carbamate formation from the corresponding alcohol **4** (Figure 2), which is accessed in two steps from compound **2** (29). Photooxidation of Cy7-β-Cou proceeds efficiently ($t_{1/2}$ = 4.9 min, Figure 4). The release of coumarin 151 occurs nearly concurrently with photooxidation at early time points, however, the yield of release only reached 14% after 20 min, and no significant additional release was observed thereafter (Figure 4B). To examine the product mixture being formed in this process, detailed mass spectrometry studies were carried out (Figure 4C). The expected intermediates Int-1 and Int-2 that derive from C2/C1' and C2'/C3' photooxidation, respectively, were observed immediately following irradiation. In following the mixture over time, we observed that Int-1 and its hydrate persists for several hours. This suggests that these species are a major and persistent component of the oxidative products derived from Cy7-β-Cou. By contrast, Int-2, disappears with apparent concurrent formation of the coumarin 151 payload. Thus, it appears the β-elimination reaction from Int-2 proceeds efficiently, but the corresponding δ-elimination from Int-1 is inefficient. In separate work, we have determined that cleavage at C2/C1' occurs preferentially to C2'/C3' cleavage in roughly a 4:1 ratio,(17) which may explain the modest yield of release.

<figure 4>

These observations suggested that it might be advantageous to pursue strategies where cyanine photooxidation occurs with high regioselectivity. To control the site of photooxidation, we considered using unsymmetrical merocyanines containing an electron-donating indolenine and an electron-deficient heterocycle partner. This approach was prompted in part by prior studies by Hahn that found that certain merocyanines undergo regioselective cleavage at the position adjacent to the more electron-rich heterocycle. (30) We designed molecules that installed a carbamate within a pendent tetrahydropyridine ring system on the electron-rich indolenine heterocycle. We anticipated that (Figure 1C) photooxidation, perhaps occurring selectively adjacent to the electron-rich indolenine

heterocycle, would produce a carbonyl intermediate poised for uncaging. For the electron deficient unit, we decided to test merocyanines containing barbituric acid and substituted-coumarin heterocycles. Merocyanines containing various barbituric acid derivatives have been used by Hahn and others as solvent-sensitive fluorophores.(31) The more recently discovered mixed courmain-indoleine merocyanines have been used in several *in vivo* biological contexts and were also chosen for their improved water solubility.(23, 32)

The synthesis of our target molecules is detailed in Figure 5. The indolenine subunit was prepared through the alkylation of indolenine **7** with glycidol triflate **8** to access epoxide **9**.(33) Epoxide **9** undergoes cyclization with triflic acid at r.t. to provide alcohol **10**.(34) The regiochemistry of the ring opening reaction to provide **10** was confirmed by COSY analysis (Figure S4). Compound **10** could be converted to the merocyanine BI-β-Cou by addition to polymethine **13**, accessed from commercial **11** and barbituic acid **12**, and carbamate formation with isocyanate **6**. Similarly, the coumarin indocyanine hybrid structure CI-β-Cou could be prepared through formylation of known **14**(23) to provide **15**, which was converted to the merocyanine through the addition of indoleine **10**, followed by carbamate formation with **6**.

<figure 5>

With access to BI-β-Cou and CI-β-Cou, we investigated their optical and uncaging properties. The absorbance/emission maxima of these two molecules, 664/693 nm and 713/729 nm (Table 1), respectively, is in line with prior molecules in these class. Photooxidation of CI-β-Cou proceeds readily with a $t_{1/2}$ of 3.4 min, with BI-β-Cou requiring longer irradiation times ($t_{1/2}$ = 20.2 min). These highly disparate photobleaching kinetics may reflect differences in aggregation state, with CI-β-Cou being mostly monomeric and BI-β-Cou being partially aggregated in the pH 7.4 PBS buffer used here (Figure S5A,B). Uncaging kinetics and yield were reasonable in both cases, with CI-β-Cou releasing

33% of coumarin 151 after 1 h and BI-β-Cou releasing 22% after 1 h (Figure 6 and Table 1). Some additional release (4-5%) is observed over the next two hours in both cases. Of note, similar yields are obtained with incubation at high temperature (e.g. 37 °C). The analysis of these reactions by mass spectrometry proved ambiguous, and, in particular, it was difficult to assess the site(s) of oxidative cleavage. We speculate that incomplete release in this case may reflect either fluorophore oxidation at some position away from desired site(s) or $^1O_2$-mediated oxidation of the uncaged amino coumarin product.(35) In total, these studies have identified scaffolds, particularly the water-soluble CI-β-Cou, that provide a versatile starting point for the development of small molecule photocages capable of uncaging a range of amine containing payloads.

<figure 6>

<Table 1>

Conclusion

In conclusion, we report efforts to use cyanine photooxidation as an initiating event for the release of aniline payloads. Our prior studies had shown that certain secondary amines could be released following photooxidative cleavage of heptamethine cyanines with useful yields and reasonable kinetic parameters. These studies illustrate that the release of amine payloads is highly subject to the electronic properties of the amine. Specifically, placing an aryl amine payload at the C4' position does not appear to interfere with cyanine photooxidation, but leads to only inefficient release (perhaps due to reduced basicity). To develop a more general approach, we have implemented a photooxidation/β-elimination reaction sequence. Embedding a carbamate functional group within the central carbocyclic ring of symmetric heptamethine cyanines improves the kinetics of the uncaging process but the release yield was only modest. Mass spectrometry studies suggest this is

likely due to the selective release from only the minor photooxidation product (C2'/C3' cleavage) and inefficient release from the major product (C2/C1' cleavage). By contrast merocyanines, and especially the coumarin containing compound, CI-β-Cou, undergoes efficient photooxidation and useful yields of uncaging. It is likely that the improved efficiency of release results from regioselective photooxidation cleavage reaction(s) to provide carbonyl intermediates that then undergo β-elimination. Additional structural optimization to improve the overall yield of release would be enabling for future efforts. In total, these studies suggest that the photooxidation/β-elimination framework provides a promising approach through which to develop NIR-activated photocages.

ACKNOWLEDGEMENTS*:* We thank Dr. Joseph Barchi, NCI Center for Cancer Research (NCI-CCR), for NMR assistance and Dr. James Kelley, NCI-CCR, for mass spectrometric analysis. This work was supported by the Intramural Research Program of the National Institutes of Health (NIH), NCI-CCR.

SUPPORTING INFORMATION

Additional supporting information may be found online in the Supporting Information section at the end of the article:

Figure S1. Coumarin 151 standard release curve.

Figure S2. Photooxidation and release of Cy7-C4-Cou.

Figure S3. Background Release Curves.

Figure S4A. Absorbance and normalized emission curves of 2 μM **Cy7-C4-Cou** (A), **Cy7-β-Cou** (B), **BI-β-Cou** (C), **CI-β-Cou** (D) in ethanol.

Figure S4B. Absorbance and normalized emission curves of 2 μM **Cy7-C4-Cou** (A), **Cy7-β-Cou** (B), **BI-β-Cou** (C), **CI-β-Cou** (D) in 5%DMSO/PBS (pH 7.

Figure S5. NMR Analysis of **10.**

^{1}H and ^{13}C NMR Spectra

FIGURE CAPTIONS

Figure 1. (A) Key Background and (B) These Studies.

Figure 2. Synthesis of Cy7-C4-Cou and Cy7-β-Cou.

Figure 3. (A) General scheme for uncaging of Cy7-C4-Cou. (B) Cyanine relative absorbance (780 nm) (left) and fluorescence (ex. 372 nm, em. 490 nm, shown as coumarin 151 concentration [μM], right) traces of a solution of Cy7-C4-Cou (2 μM, pH 7.4 PBS w/ 5% DMSO) that was irradiated (red boxes, 780 nm ± 20 nm) or not and (black boxes).

Figure 4: (A) General scheme for uncaging from Cy7-β-Cou. (B) Cyanine absorbance (780 nm) (left) and coumarin fluorescence readings (ex. 372 nm, em. 490 nm, shown as concentration [μM], right) of a solution of Cy7-β-Cou (2 μM, pH 7.4 PBS w/ 5% DMSO) that was irradiated (red boxes, 780 nm ± 20 nm) or not and (black boxes). (C) Mass spectrometry analysis following irradiation of solution Cy7-β-Cou (2 μM in H_2O).

Figure 5. Synthesis of BI-β-Cou and CI-β-Cou.

Figure 6: Uncaging of BI-β-Cou (blue) and CI-β-Cou (red). Absorbance (at the cyanine λ_{max}) and fluorescence traces (ex. 372 nm, em. 490 nm, shown as concentration [μM] of coumarin 151) for solutions of BI-β-Cou (blue) and CI-β-Cou (red) in pH 7.4 PBS w/ 5% DMSO following irradiation (solid boxes, 660 nm ± 20 nm for BI-β-Cou and 690 nm ± 20 nm for CI-β-Cou) or not (empty boxes).

Table 1. Key parameters.

Cmp.	λ_{abs} **(nm)**[a]	λ_{em} **(nm)**[a]	ε^{abs} **($M^{-1}cm-1$)**[a]	**Cyanine $t_{1/2}$ (min)**[b]	**Uncaging yield (%)**[b]
Cy-C4-Cou	779	803	2.38×10^5	5.7	0.6 ± 0.04[c] 8.0 ± 0.1[d]
Cy-β-Cou	781	805	2.99×10^5	4.9	16 ± 0.2[c]
BI-β-Cou	664	693	1.61×10^5	20.2	22 ± 1.0[c]
CI-β-Cou	713	729	1.21×10^5	3.4	33 ± 0.4[c]

[a] Measured in EtOH.

[b] As determined in Figures 3, 4, and 6.

[c] Yield after 1 h at room temperature.

[d] Yield after 24 h at 37 °C.

References

1. Lee, H. M., D. R. Larson and D. S. Lawrence (2009) Illuminating the Chemistry of Life: Design, Synthesis, and Applications of "Caged" and Related Photoresponsive Compounds. *Acs Chem Biol* **4,** 409-427.

2. Ankenbruck, N., T. Courtney, Y. Naro and A. Deiters (2018) Optochemical Control of Biological Processes in Cells and Animals. *Angewandte Chemie* **57,** 2768-2798.

3. Solomek, T., J. Wirz and P. Klan (2015) Searching for Improved Photoreleasing Abilities of Organic Molecules. *Acc Chem Res* **48,** 3064-3072.

4. Bio, M., G. Nkepang and Y. You (2012) Click and photo-unclick chemistry of aminoacrylate for visible light-triggered drug release. *Chem Commun* **48,** 6517-6519.

5. Slanina, T., P. Shrestha, E. Palao, D. Kand, J. A. Peterson, A. S. Dutton, N. Rubinstein, R. Weinstain, A. H. Winter and P. Klan (2017) In Search of the Perfect Photocage: Structure-Reactivity Relationships in meso-Methyl BODIPY Photoremovable Protecting Groups. *J Am Chem Soc* **139,** 15168-15175.

6. Peterson, J. A., C. Wijesooriya, E. J. Gehrmann, K. M. Mahoney, P. P. Goswami, T. R. Albright, A. Syed, A. S. Dutton, E. A. Smith and A. H. Winter (2018) Family of BODIPY Photocages Cleaved by Single Photons of Visible/Near-Infrared Light. *J Am Chem Soc* **140,** 7343-7346.

7. Shell, T. A., J. R. Shell, Z. L. Rodgers and D. S. Lawrence (2014) Tunable Visible and Near-IR Photoactivation of Light-Responsive Compounds by Using Fluorophores as Light-Capturing Antennas. *Angew Chem Int Edit* **53,** 875-878.

8. Anderson, E. D., A. P. Gorka and M. J. Schnermann (2016) Near-infrared uncaging or photosensitizing dictated by oxygen tension. *Nat Commun* **7,** 13378.

9. Wang, X. and J. A. Kalow (2018) Rapid Aqueous Photouncaging by Red Light. *Org Lett* **20,** 1716-1719.

10. Ghosh, G., S. J. Belh, C. Chiemezie, N. Walalawela, A. A. Ghogare, M. Vignoni, A. H. Thomas, S. A. McFarland, E. M. Greer and A. Greer (2018) S,S-Chiral Linker Induced U Shape with a Syn-facial Sensitizer and Photocleavable Ethene Group. *Photochem Photobiol*.

11. Walton, D. P. and D. A. Dougherty (2017) A General Strategy for Visible-Light Decaging Based on the Quinone Trimethyl Lock. *J Am Chem Soc* **139,** 4655-4658.

12. Fomina, N., J. Sankaranarayanan and A. Almutairi (2012) Photochemical mechanisms of light-triggered release from nanocarriers. *Adv Drug Deliv Rev* **64,** 1005-1020.

13. Alabugin, A. (2018) Near IR Photochemistry for Biology: Exploiting the Optical Window of Tissue. Photochemisty and Photobiology https://doi.org/10.1111/php.13068

14. Gorka, A. P., R. R. Nani, J. Zhu, S. Mackem and M. J. Schnermann (2014) A Near-IR Uncaging Strategy Based on Cyanine Photochemistry. *Journal of the American Chemical Society* **136,** 14153-14159.

15. Gorka, A. P. and M. J. Schnermann (2016) Harnessing cyanine photooxidation: from slowing photobleaching to near-IR uncaging. *Curr Opin Chem Biol* **33,** 117-125.

16. Gorka, A. P., T. Yamamoto, J. J. Zhu and M. J. Schnermann (2018) Cyanine Photocages Enable Spatial Control of Inducible Cre-Mediated Recombination. *Chembiochem : a European journal of chemical biology* **19,** 1239-1243.

17. Nani, R. R., J. A. Kelley, J. Ivanic and M. J. Schnermann (2015) Reactive Species Involved in the Regioselective Photooxidation of Heptamethine Cyanines. *Chem Sci* **6,** 6556-6563.

18. Nani, R. R., A. P. Gorka, T. Nagaya, H. Kobayashi and M. J. Schnermann (2015) Near-IR Light-Mediated Cleavage of Antibody-Drug Conjugates Using Cyanine Photocages. *Angewandte Chemie* **54,** 13635-13638.

19. Nani, R. R., A. P. Gorka, T. Nagaya, T. Yamamoto, J. Ivanic, H. Kobayashi and M. J. Schnermann (2017) In Vivo Activation of Duocarmycin-Antibody Conjugates by Near-Infrared Light. *Acs Central Sci* **3,** 329-337.

20. Deiters, A. (2009) Light activation as a method of regulating and studying gene expression. *Curr Opin Chem Biol* **13,** 678-686.

21. Ryu, K. A., L. Stutts, J. K. Tom, R. J. Mancini and A. P. Esser-Kahn (2014) Stimulation of innate immune cells by light-activated TLR7/8 agonists. *J Am Chem Soc* **136,** 10823-10825.

22. Mujumdar, R. B., L. A. Ernst, S. R. Mujumdar, C. J. Lewis and A. S. Waggoner (1993) Cyanine dye labeling reagents: sulfoindocyanine succinimidyl esters. *Bioconjug Chem* **4,** 105-111.

23. Yuan, L., W. Lin, Y. Yang and H. Chen (2012) A unique class of near-infrared functional fluorescent dyes with carboxylic-acid-modulated fluorescence ON/OFF switching: rational design, synthesis, optical properties, theoretical calculations, and applications for fluorescence imaging in living animals. *J Am Chem Soc* **134,** 1200-1211.

24. Pascal, S., A. Haefele, C. Monnereau, A. Charaf-Eddin, D. Jacquemin, B. Le Guennic, C. Andraud and O. Maury (2014) Expanding the Polymethine Paradigm: Evidence for the Contribution of a Bis-Dipolar Electronic Structure. *J Phys Chem A* **118,** 4038-4047.

25. Mahajan, S. S., E. Deu, E. M. Lauterwasser, M. J. Leyva, J. A. Ellman, M. Bogyo and A. R. Renslo (2011) A fragmenting hybrid approach for targeted delivery of multiple therapeutic agents to the malaria parasite. *ChemMedChem* **6,** 415-419.

26. Santi, D. V., E. L. Schneider, R. Reid, L. Robinson and G. W. Ashley (2012) Predictable and tunable half-life extension of therapeutic agents by controlled chemical release from macromolecular conjugates. *Proc Natl Acad Sci U S A* **109,** 6211-6216.

27. Tu, J. L., M. H. Xu, S. Parvez, R. T. Peterson and R. M. Franzini (2018) Bioorthogonal Removal of 3-Isocyanopropyl Groups Enables the Controlled Release of Fluorophores and Drugs in Vivo. *Journal of the American Chemical Society* **140,** 8410-8414.

28. Spangler, B., C. W. Morgan, S. D. Fontaine, M. N. Vander Wal, C. J. Chang, J. A. Wells and A. R. Renslo (2016) A reactivity-based probe of the intracellular labile ferrous iron pool. *Nature Chemical Biology* **12,** 680-+.

29. Yang, Z., J. H. Lee, H. M. Jeon, J. H. Han, N. Park, Y. He, H. Lee, K. S. Hong, C. Kang and J. S. Kim (2013) Folate-Based Near-Infrared Fluorescent Theranostic Gemcitabine Delivery. *Journal of the American Chemical Society* **135,** 11657-11662.

30. Toutchkine, A., D. V. Nguyen and K. M. Hahn (2007) Merocyanine dyes with improved photostability. *Organic Letters* **9,** 2775-2777.

31. Toutchkine, A., V. Kraynov and K. Hahn (2003) Solvent-sensitive dyes to report protein conformational changes in living cells. *Journal of the American Chemical Society* **125,** 4132-4145.

32. Sun, W., S. Guo, C. Hu, J. Fan and X. Peng (2016) Recent Development of Chemosensors Based on Cyanine Platforms. *Chem Rev* **116,** 7768-7817.

33. Baldwin, J. J., D. E. Mcclure, D. M. Gross and M. Williams (1982) Use of (S)-(Trifloxymethyl)Oxirane in the Synthesis of a Chiral Beta-Adrenoceptor Antagonist, (R) and (S)-9-[[3-(Tert-Butylamino)-2-Hydroxypropyl]Oximino]Fluorene. *J Med Chem* **25,** 931-936.

34. Yang, L., Q. Y. Zheng, D. X. Wang, Z. T. Huang and M. X. Wang (2008) Reversal of nucleophilicity of enamides in water: control of cyclization pathways by reaction media for the orthogonal synthesis of dihydropyridinone and pyrrolidinone Clausena alkaloids. *Org Lett* **10,** 2461-2464.

35. Al-Nu'airat, J., M. Altarawneh, X. Gao, P. R. Westmoreland and B. Z. Dlugogorski (2017) Reaction of Aniline with Singlet Oxygen (O2(1)Deltag). *J Phys Chem A* **121,** 3199-3206.

A. Prior Work -
Cyanine Photooxidation to Initate Phenol Release

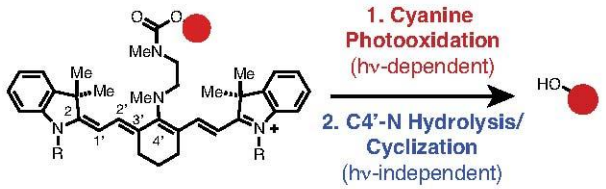

B. These Studies -
Cyanine Photooxidation to Initate Aniline Release

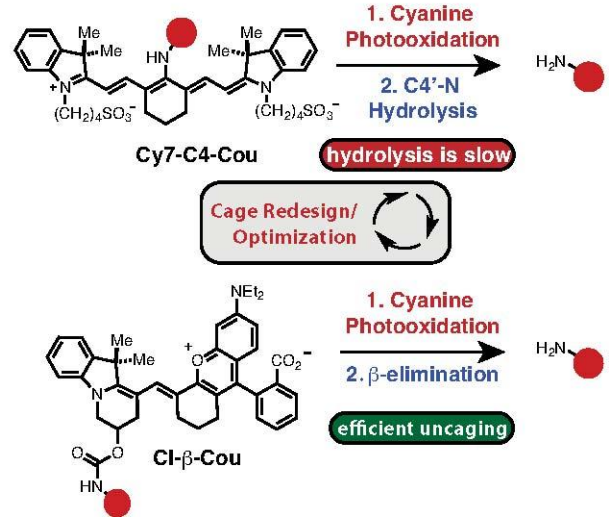

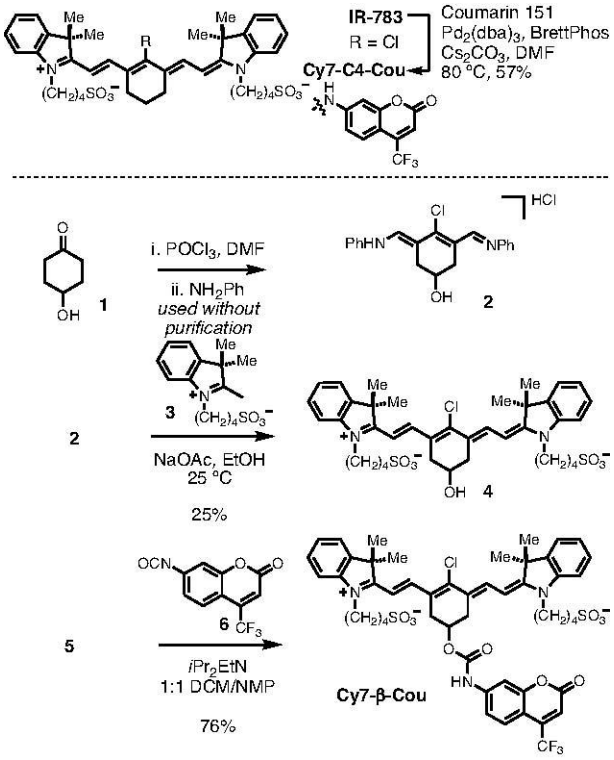

A. Release of Directly Attached Aryl Amine

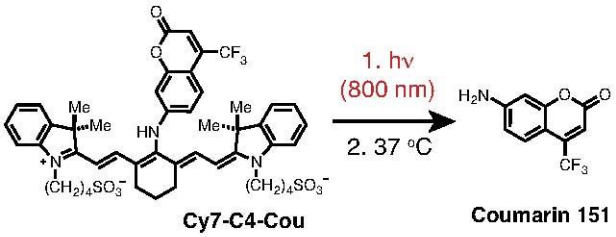

B. Photooxidation and Release